Advances in Applied Mathematics and Mechanics
Adv. Appl. Math. Mech., Vol. **13**, No. 3, pp. 701-723

DOI: 10.4208/aamm.OA-2019-0328
June 2021

Anisotropic Yield Criterion for Metals Exhibiting Tension–Compression Asymmetry

Lei Chen[1], Jian Zhang[1,2,*] and Hongjian Zhang[3]

[1] *Faculty of Civil Engineering and Mechanics, Jiangsu University, Zhenjiang, Jiangsu 212013, China*
[2] *National Center for International Research on Structural Health Management of Critical Components, Jiangsu University, Zhenjiang, Jiangsu 212013, China*
[3] *College of Energy and Power Engineering, Nanjing University of Aeronautics and Astronautics, Nanjing, Jiangsu 210016, China*

Received 12 November 2019; Accepted (in revised version) 2 July 2020

Abstract. The present study is devoted to developing a yield criterion that can model both the yielding asymmetry and plastic anisotropy of pressure-insensitive metals. First, a new isotropic yield criterion which can model the yielding asymmetry of pressure-insensitive metals is proposed. The main advantage of the proposed criterion is that it leads to a good approximation of yield loci calculated by the Taylor-Bishop-Hill crystal plasticity model. Further, the isotropic criterion is extended to orthotropy to take plastic anisotropy into account. The new anisotropic criterion is general and can be used in three-dimensional stresses. The coefficients of the criterion are determined by an error minimization procedure. Applications of the proposed theory to a hexagonal close packed (HCP) magnesium, a Cu-Al-Be shape memory alloy and a Ni3Al based intermetallic alloy show that the proposed theory can describe well the plastic anisotropy and yielding asymmetry of metals and the transformation onset of the shape memory alloy, showing excellent predictive ability and flexibility.

AMS subject classifications: 74C05, 74D10, 74E10

Key words: Yield criterion, yielding asymmetry, plastic anisotropy, magnesium alloy, shape memory alloy, intermetallic alloy.

1 Introduction

In modern industry, virtual manufacturing technology is one of the most efficient methods to reduce production cycles and improve the quality of products. As a part of virtual

*Corresponding author.
Email: jianzhang@ujs.edu.cn (J. Zhang)

manufacturing, numerical simulation of metal forming processes has always been a research hotspot [1, 2]. The traditional manufacturing process analysis and mold design rely mainly on the designer's experience. In order to avoid defects such as wrinkles and cracks, it is necessary to continuously test and repair molds, which results in long mold production cycles and low efficiency. With the rapid development of computer technology, metal sheet forming is gradually assisted by numerical simulations, which can not only reduce the cost of mold testing, but also shorten the production cycles [3]. This is a great progress in the field of metal plastic forming. It is generally known that the plastic analysis of metal forming processes depends on the yield criterion and associated plastic flow rules employed. In order to improve the accuracy of numerical plastic forming simulations, it is essential to develop appropriate yield criteria involved. Given their importance to plastic forming analysis, tremendous yield criteria for different metals have been proposed by researchers at home and abroad.

For isotropic metals, the von Mises and Tresca criteria are the ones most used to predict the plastic behavior of materials. And the von Mises criterion has been widely implemented in commercial FEM software packages such as ANSYS and ABAQUS. However, there are numerous other isotropic criteria in literature [4–6]. Actually, research on yield criteria for isotropic metals has been done quite thoroughly and the plastic forming simulations are accurate enough in most cases. However, due to their complicated plastic behavior, yield criteria for anisotropic metals are far from being thoroughly studied. In general, the pre-machined or pre-rolled metal sheet exhibits significant anisotropy, which has significant effects on the plastic forming process. In order to model the plastic behavior of anisotropic materials, Hill proposed the first orthotropic yield criterion, which reduces to von Mises criterion for isotropic conditions [7]. So far, because of its simplicity, this famous criterion has been widely used in analytical or numerical simulations of forming processes. Later, tremendous anisotropic yield cri-teria have been proposed. For reviews concerning yield criteria of metals one may refer to [8,9]. Subsequently, outstanding contributions have been made by Hill [10–13], Hosford [14–17] and Barlat [18–21]. For latest research concerning yielding behavior of solids, one may refer to [22–27]. For metallic materials, slip of dislocations and twinning are the main plastic deformation mechanisms. For both conditions, shear strains occurred on certain crystallographic planes and along certain directions. If the shear mechanism is reversible, yielding is insensitive to the sign of the stress but is only related to the magnitude of the re-solved shear stress. Thus, we get equal tensile yield stress and compressive yield stress. Most yield criteria in literature, expressed by even functions of the stress components, are based on the hypothesis of tension-compression asymmetry. This is true for metals deforming by reversible shear mechanism. However, not all metallic materials are tension-compression symmetric. Due to the directionality of twinning, a remarkable strength differential (SD) effect is observed in HCP materials at low strain levels. In general, the yield stress in tension is much higher than that in compression [17]. For Ll_2-long-range ordered intermetallic alloy, SD effect is observed for its violation of Schmid's law [28]. To model the strength differential effect of pressure insensitive metals, yield functions that can describe SD effects of metals have been proposed in recent years [29–33]. Those criteria have gained a lot of attention and some have been used to describe the SD effects of engineering materials [34–37].

Compared to the tremendous anisotropic yield functions proposed for materials with equal tension and compression, criteria that can model both plastic anisotropy and yielding asymmetry are still lacking. In the next section, a new isotropic yield criterion, which can model the SD effects of pressure insensitive metals, will be suggested.

2 Proposed isotropic yield criterion

Recently, an isotropic yield function in terms of J_2 and J_3 has been proposed by Cazacu [38]

$$f \equiv J_2^4 - \alpha J_2 J_3^2 = \tau_Y^8. \tag{2.1}$$

Here, $J_2 = trS^2/3$ represents the second invariant of the stress deviator $\boldsymbol{S}$, and $J_3 = trS^3/3$ represents the third invariant of the stress deviator $\boldsymbol{S}$ (tr represents the trace operator $tr(A) = \sum_{k=1}^{3} A_{kk}$); τ_Y is the shear strength, which can be approximated as $\tau_Y = \sigma_0^T/\sqrt{3}$ [39], and α is a material constant. Of particular interest here, a product term of J_2 and J_3 was introduced. The yield locus predicted by Cazacu's criterion shows very good agreement with the Taylor-Bishop-Hill polycrystalline simulations for randomly oriented face-centered-cubic (FCC) polycrystals [38].

As Cazacu's criterion (Eq. (2.1)) is an even function of the components of the stress tensor, it cannot capture asymmetry in yielding. The success of Cazacu's criterion for predicting the plastic response of FCC polycrystals gives confidence in extending it to tension-compression asymmetry conditions. In order to capture asymmetry in yielding of materials, the following isotropic function is proposed:

$$\phi \equiv J_2^{5/2} - \alpha J_2 J_3 = \tau_Y^5. \tag{2.2}$$

The physical significance of α can be interpreted by uniaxial loading tests. Consider a uniaxial tension test, yielding occurs when $\sigma_1 = \sigma_t$, $\sigma_2 = \sigma_3 = 0$. Substituting these stresses into Eq. (2.2), we get

$$\sigma_t = \tau_Y \left(\frac{81\sqrt{3}}{9 - 2\sqrt{3}\alpha} \right)^{1/5}. \tag{2.3}$$

Suppose σ_c is yield stress in uniaxial compression such that

$$\sigma_c = \tau_Y \left(\frac{81\sqrt{3}}{9 + 2\sqrt{3}\alpha} \right)^{1/5}. \tag{2.4}$$

Hence,

$$\alpha=\frac{3\sqrt{3}}{2}\left(\frac{\sigma_t^5-\sigma_c^5}{\sigma_t^5+\sigma_c^5}\right)^{1/5} \tag{2.5}$$

for

$$\sigma_t>\sigma_c>0\Rightarrow\alpha\in\left(0,\frac{3\sqrt{3}}{2}\right),$$

for

$$0<\sigma_t<\sigma_c\Rightarrow\alpha\in\left(-\frac{3\sqrt{3}}{2},0\right). \tag{2.6}$$

For materials with equal tensile and compressive yield stresses, i.e., $\alpha=0$, the suggested yield function (2.2) is identical with von Mises criterion. For the yield function to be convex, α is limited to a given numerical range: $\alpha\in(-2.25,2.25)$.

For a state of plane stress, Eq. (2.2) is simplified as

$$\begin{aligned}&\left[\frac{1}{3}\left({\sigma_1}^2-\sigma_1\sigma_2+{\sigma_2}^2\right)\right]^{5/2}-\frac{\alpha}{81}\left({\sigma_1}^2-\sigma_1\sigma_2+{\sigma_2}^2\right)\\&\quad\times\left[2{\sigma_1}^3+2{\sigma_2}^3-3(\sigma_1+\sigma_2)\sigma_1\sigma_2\right]=\tau_Y^5.\end{aligned} \tag{2.7}$$

For any $\alpha\neq0$, the yield locus of Eq. (2.7) is a "triangle" with rounded corners. As a demonstration, Fig. 1 shows the plane stress yield loci of Eq. (2.7) obtained corresponding to $\sigma t/\sigma_c=4/5,1,6/5$, respectively. These ratios correspond to $\alpha=-1.316,0$ (von Mises), 1.108, respectively.

Based on combined tension and torsion tests, Taylor and Quinney [40] pointed that the third invariant of the stress deviators has effect on the yielding behavior of metals. Considering the stress state of combined tension and torsion, suppose $\sigma_{11}=\sigma$, $\sigma_{12}=\tau$ and all other components of stress tensor are zero, and the yield locus of the proposed criterion in (σ,τ) plane is given by

$$\left[\frac{1}{3}\left(\sigma^2+3\tau^2\right)\right]^{5/2}-\frac{\alpha}{81}\left(\sigma^2+3\tau^2\right)\left(2\sigma^3+9\tau^2\sigma\right)={\tau_Y}^5. \tag{2.8}$$

Fig. 2 displays the yield loci in the tension-torsion plane $(\sigma_{11}/\bar{\sigma},\sigma_{12}/\bar{\sigma})$ of the Tresca criterion and the proposed criterion (Eq. (2.8)) according to $\sigma_t/\sigma_c=4/5$, 1 (von Mises) and $6/5$, respectively. It can be seen that for $\sigma_t/\sigma_c\neq1$ the yield locus of the proposed criterion departures sharply from that of the von Mises ellipse.

Tricomponent plane stress yield surface for isotropic FCC metals calculated by Taylor-Bishop-Hill crystal plasticity model [41] shows that a coupling should exist between

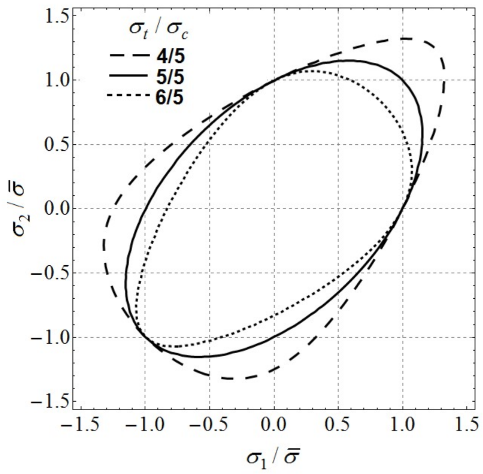

Figure 1: Yield loci predicted by the proposed isotropic yield function, according to $\sigma_t/\sigma_c = 4/5$, 5/5 (von Mises), 6/5.

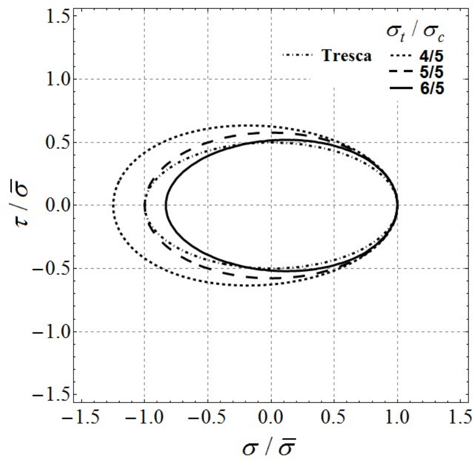

Figure 2: Yield loci predicted by Tresca criterion and the proposed isotropic yield function in the (σ,τ) plane for $\sigma_t/\sigma_c = 4/5$, 5/5 (von Mises), 6/5.

shear and normal components of stress. Fig. 3 shows the section of the yield surface of the proposed isotropic yield function with planes parallel to the $\sigma_{xx}/\bar{\sigma}$,$\sigma_{yy}/\bar{\sigma}$ plane for different values of $S = \sigma_{xy}/\bar{\sigma}$. For materials with tension/compression symmetry $(\alpha = 0)$, Eq. (2.2) reduces to von Mises criterion and there is no coupling between shear and normal stress components. Therefore, the yield loci (dotted lines) in Fig. 3(a) exhibit the same shape for different shear stresses. For materials with tension/compression asymmetry $(\alpha \neq 0)$, the yield loci predicted by Eq. (2.2) do not exhibit the same shape for different

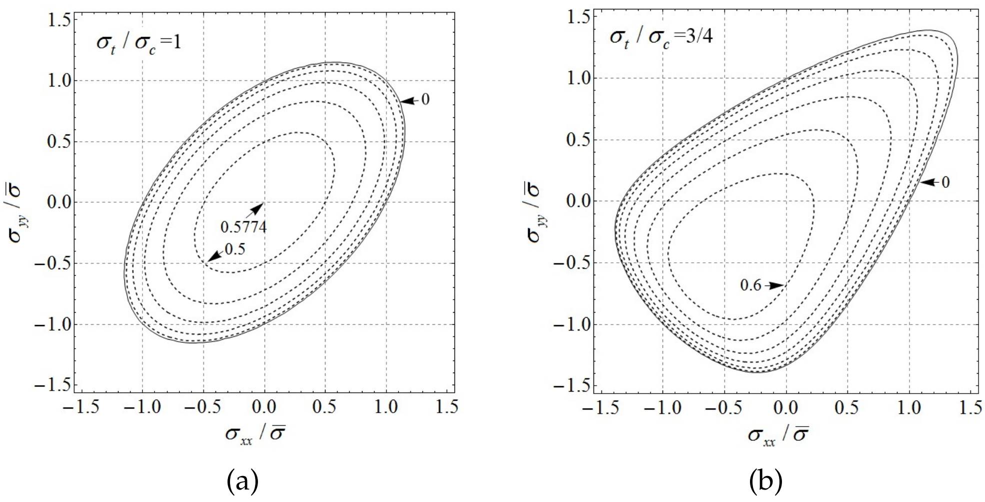

Figure 3: Tricomponent plane stress yield loci of the proposed isotropic yield function. The dotted line represents the section of the yield surface by a plane parallel to $(\sigma_{xx}/\bar{\sigma},\sigma_{yy}/\bar{\sigma})$ for different value $S=\sigma_{xy}/\bar{\sigma}$ (constant normalized shear stresses S every 0.1). (a) $\sigma_t/\sigma_c=1$ (von Mises), (b) $\sigma_t/\sigma_c=3/4$.

shear stresses, demonstrating couplings between shear and normal components of stress (see Fig. 3(b)).

In order to check the predictive capability of the proposed yield function, the yield loci of Eq. (2.2) are constructed and compared with the polycrystal calculations of FCC polycrystals by Hosford and Allen [16] based on a generalization of the Taylor-Bishop-Hill model [41]. The FCC metals, with randomly oriented polycrystals, are deformed by $\{111\}$ $\{11\bar{2}\}$ twinning. The only parameter in the proposed criterion is α, which is determined by the ratio of σ_t/σ_c (see Eq. (2.5)). A value of σ_t/σ_c calculated for randomly oriented FCC polycrystals by Hosford and Allen is 0.78, to which the constant $\alpha=-1.427$. Fig. 4 shows the predicted yield locus of Eq. (2.2) for $\alpha=-1.427$ (solid curve) and polycrystalline model calculated results (full circles) by Hosford and Allen [16]. Note that the proposed criterion could reproduce the yield locus of FCC polycrystals obtained by polycrystalline calculations. Fig. 4 also shows the results of the comparison for body-centered-cubic (BCC) polycrystals, which deform solely by $\{112\}$ $\{\bar{1}\bar{1}\bar{1}\}$ twinning. Dashed curve and open circles represent the yield locus of Eq. (2.2) and the polycrystal model, respectively. The ratio of σ_t/σ_c predicted by polycrystalline model is 1.28 for BCC structured metals, to which the value of α in the proposed criterion is 1.427. The comparison shows that the proposed isotropic criterion can accurately model the yield stresses obtained by polycrystalline model.

In general, the proposed isotropic criterion, which contains a product term of J_2 and J_3, could describe very well the asymmetry in yielding of both FCC and BCC structured metals deformed by twinning. To model both the yielding asymmetry and plastic

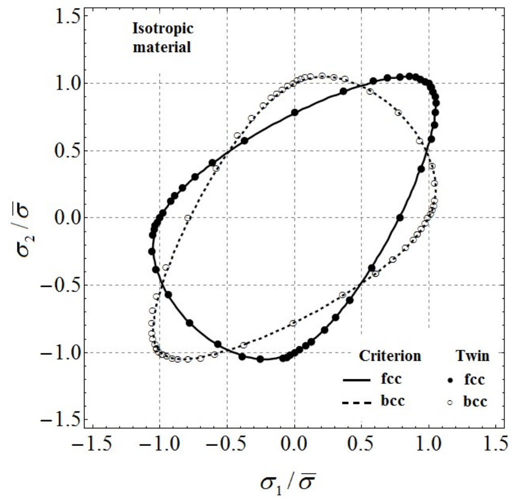

Figure 4: Comparison between plane stress yield loci of the proposed isotropic yield function and polycrystalline model (Hosford and Allen [16]): (a) FCC ($\sigma_t/\sigma_c=0.78$ for which $\alpha=-1.427$) (b) BCC (($\sigma_t/\sigma_c=1.28$ for which $\alpha=1.427$).

anisotropy of metallic materials, we will extend the proposed theory to orthotropy in the next section.

3 Extension of the isotropic yield function and parameter identification

3.1 Extension of the isotropic yield function to orthotropy

In the following we will extend the proposed isotropic criterion (Eq. (2.2)) to orthotropy, so that it can describe both plastic anisotropy and yield asymmetry of pressure insensitive metals. There are several ways available to extend an isotropic criterion to anisotropy, such as the method of linearly transformed stress tensors [42,43] and the "isotropy plasticity equivalent" (IPE) method introduced by Karafillis and Boyce [44]. Here we use the approach that consists of using the representation theorems to construct generalizations of anisotropy conditions of classic invariants of J_2 and J_3. This approach was first introduced by Cazacu and Barlat [45], which could include any type of anisotropy. The orthotropic generalizations of the second and third invariant of the stress deviator, denoted by J_2^0 and J_3^0 are:

$$\begin{aligned} J_2^0=&\frac{a_1}{6}(\sigma_{yy}-\sigma_{zz})^2+\frac{a_2}{6}(\sigma_{zz}-\sigma_{xx})^2+\frac{a_3}{6}(\sigma_{xx}-\sigma_{yy})^2\\ &+a_4\sigma_{yz}^2+a_5\sigma_{zx}^2+a_6\sigma_{xy}^2, \end{aligned} \tag{3.1a}$$

$$\begin{aligned}
J_3^0=&\frac{1}{27}(b_1+b_2)\sigma_{xx}^3+\frac{1}{27}(b_3+b_4)\sigma_{yy}^3+\frac{1}{27}[2(b_1+b_4)-b_2-b_3]\sigma_{zz}^3\\
&-\frac{1}{9}(b_1\sigma_{yy}+b_2\sigma_{zz})\sigma_{xx}^2-\frac{1}{9}(b_3\sigma_{zz}+b_4\sigma_{xx})\sigma_{yy}^2\\
&-\frac{1}{9}\left[(b_1-b_2+b_4)\sigma_{xx}+(b_1-b_3+b_4)\sigma_{yy}\right]\sigma_{zz}^2\\
&+\frac{2}{9}(b_1+b_4)\sigma_{xx}\sigma_{yy}\sigma_{zz}-\frac{\sigma_{yz}^2}{3}\left[(b_6+b_7)\sigma_{xx}-b_6\sigma_{yy}-b_7\sigma_{zz}\right]\\
&-\frac{\sigma_{zx}^2}{3}\left[2b_9\sigma_{yy}-b_8\sigma_{zz}-(2b_9-b_8)\sigma_{xx}\right]\\
&-\frac{\sigma_{xy}^2}{3}\left[2b_{10}\sigma_{zz}-b_5\sigma_{yy}-(2b_{10}-b_5)\sigma_{xx}\right]+2b_{11}\sigma_{yz}\sigma_{zx}\sigma_{xy},
\end{aligned}\tag{3.1b}$$

where x, y, and z coincide with the three principal axes of anisotropy, such as the rolling direction, the long transverse direction, and the short transverse direction, respectively. And a_k $(k=1,\cdots,6)$ and b_k $(k=1,\cdots,11)$ are constants characteristic of the current state of anisotropy. It's easy to prove that, for any p and σ,

$$J_2^0(\sigma+pI)=J_2^0(\sigma),\quad J_3^0(\sigma+pI)=J_3^0(\sigma),\tag{3.2}$$

which implies that J_2^0 and J_3^0 are insensitive to hydrostatic pressure. Also, J_2^0 and J_3^0 are invariants to any transformation belonging to the symmetry group of the material. If all the coefficients a_k $(k=1,\cdots,6)$ are set to unity, J_2^0 reduces to J_2. While all the coefficients b_k $(k=1,\cdots,11)$ reduce to unity for isotropic conditions, J_3^0 reduces to J_3. Using the approach discussed above, the following orthotropic yield criterion is derived based on Eq. (2.2)

$$\Phi\equiv\left(J_2^0\right)^{5/2}-\alpha J_2^0J_3^0=\tau_Y^5.\tag{3.3}$$

Obviously, the proposed orthotropic criterion is insensitive to hydrostatic pressure, which is consistent with the hypothesis that hydrostatic pressure does not cause plastic deformation of metals.

It should be noted that extension of isotropic yield function using linear transformation of the Cauchy stress tensor may have convexity problems [46]. For anisotropic yield function containing a great deal of parameters with complex mathematical expression, the convexity requirement would not be easy to check. In this case, the convexity of yield criterion for a specific material can be investigated by graphical method. The convexity of the proposed yield function has been checked for materials applied in this paper, as in the Appendix.

For a thin sheet perpendicular to the z axis and in a condition of plane stress

$(\sigma_{xx},\sigma_{yy},\sigma_{xy})$ the proposed criterion (Eq. (3.3)) is expressed as

$$\begin{aligned}\Phi\equiv&\left[\frac{1}{6}(a_1+a_3)\sigma_{xx}^2-\frac{a_1}{3}\sigma_{xx}\sigma_{yy}+\frac{1}{6}(a_1+a_2)\sigma_{yy}^2+a_4\tau_{xy}^2\right]^{5/2}\\&-\alpha\left[\frac{1}{6}(a_1+a_3)\sigma_{xx}^2-\frac{a_1}{3}\sigma_{xx}\sigma_{yy}+\frac{1}{6}(a_1+a_2)\sigma_{yy}^2+a_4\tau_{xy}^2\right]\\&\times\left\{\begin{array}{c}\frac{1}{27}(b_1+b_2)\sigma_{xx}^3+\frac{1}{27}(b_3+b_4)\sigma_{yy}^3\\-\frac{1}{9}(b_1\sigma_{xx}+b_4\sigma_{yy})\sigma_{xx}\sigma_{yy}\\-\frac{1}{3}\sigma_{xy}^2\left[(b_5-2b_{10})\sigma_{xx}-b_5\sigma_{yy}\right]\end{array}\right\}=\tau_Y^5.\end{aligned}\tag{3.4}$$

In particular, the section of the yield locus with $\sigma_{xy}=0$ is

$$\begin{aligned}&\left[\frac{1}{6}(a_1+a_3)\sigma_1^2-\frac{a_1}{3}\sigma_1\sigma_2+\frac{1}{6}(a_1+a_2)\sigma_2^2\right]^{5/2}\\&-\alpha\left[\frac{1}{6}(a_1+a_3)\sigma_1^2-\frac{a_1}{3}\sigma_1\sigma_2+\frac{1}{6}(a_1+a_2)\sigma_2^2\right]\\&\times\left\{\begin{array}{c}\frac{1}{27}(b_1+b_2)\sigma_1^3+\frac{1}{27}(b_3+b_4)\sigma_2^3\\-\frac{1}{9}(b_1\sigma_1+b_4\sigma_2)\sigma_1\sigma_2\end{array}\right\}=\tau_Y^5.\end{aligned}\tag{3.5}$$

Suppose a uniaxial tension σ_θ directed at an angle θ with the x axis, then

$$\left\{\begin{array}{l}\sigma_{xx}=\sigma_\theta\cos^2\theta,\\\sigma_{yy}=\sigma_\theta\sin^2\theta,\\\sigma_{xy}=\sigma_\theta\sin\theta\cos\theta.\end{array}\right.\tag{3.6}$$

If σ_θ^T and σ_θ^C are the yield stresses of the tensile and compression test specimens under uniaxial loading. Substituting (3.6) into (3.4), it follows that

$$\sigma_\theta^T=\tau_Y\left\{\begin{array}{c}\left[\begin{array}{c}\frac{1}{6}(a_1+a_3)\cos^4\theta+(a_4-a_1/3)\cos^2\theta\sin^2\theta\\+\frac{1}{6}(a_1+a_2)\sin^4\theta\end{array}\right]^{5/2}\\-\alpha\left[\begin{array}{c}\frac{1}{6}(a_1+a_3)\cos^4\theta+(a_4-a_1/3)\cos^2\theta\sin^2\theta\\+\frac{1}{6}(a_1+a_2)\sin^4\theta\end{array}\right]\\\left\{\begin{array}{c}\frac{1}{27}(b_1+b_2)\cos^6\theta+\frac{1}{27}(b_3+b_4)\sin^6\theta\\-\frac{1}{9}\left[\begin{array}{c}(b_1+3b_5-6b_{10})\cos^2\theta\\+(b_4-3b_5)\sin^2\theta\end{array}\right]\sin^2\theta\cos^2\theta\end{array}\right\}\end{array}\right\}^{-1/5},\tag{3.7a}$$

$$\sigma_\theta^C=\tau_y\left\{\frac{\left[\begin{array}{l}\frac{1}{6}(a_1+a_3)\cos^4\theta+(a_4-a_1/3)\cos^2\theta\sin^2\theta\\+\frac{1}{6}(a_1+a_2)\sin^4\theta\end{array}\right]^{5/2}+\alpha\left[\begin{array}{l}\frac{1}{6}(a_1+a_3)\cos^4\theta+(a_4-a_1/3)\cos^2\theta\sin^2\theta\\+\frac{1}{6}(a_1+a_2)\sin^4\theta\end{array}\right]}{\left\{\begin{array}{l}\frac{1}{27}(b_1+b_2)\cos^6\theta+\frac{1}{27}(b_3+b_4)\sin^6\theta\\-\frac{1}{9}\left[\begin{array}{l}(b_1+3b_5-6b_{10})\cos^2\theta\\+(b_4-3b_5)\sin^2\theta\end{array}\right]\sin^2\theta\cos^2\theta\end{array}\right\}}\right\}^{-1/5}. \tag{3.7b}$$

In particular,

$$\sigma_0^T=\tau_Y\left[\left(\frac{a_1+a_3}{6}\right)^{5/2}-\alpha\left(\frac{a_1+a_3}{6}\right)\left(\frac{b_1+b_2}{27}\right)\right]^{-1/5}, \tag{3.8a}$$

$$\sigma_{45}^T=\tau_Y\left[\begin{array}{c}\left(\frac{a_2+a_3-6a_4}{24}\right)^{5/2}-\frac{\alpha}{5184}(a_2+a_3-6a_4)\\(b_2+b_3-2b_1-2b_4-18b_{10})\end{array}\right]^{-1/5}, \tag{3.8b}$$

$$\sigma_{90}^T=\tau_Y\left[\left(\frac{a_1+a_2}{6}\right)^{5/2}-\alpha\left(\frac{a_1+a_2}{6}\right)\left(\frac{b_3+b_4}{27}\right)\right]^{-1/5}, \tag{3.8c}$$

$$\sigma_0^C=\tau_Y\left[\left(\frac{a_1+a_3}{6}\right)^{5/2}+\alpha\left(\frac{a_1+a_3}{6}\right)\left(\frac{b_1+b_2}{27}\right)\right]^{-1/5}, \tag{3.8d}$$

$$\sigma_{45}^C=\tau_Y\left[\begin{array}{c}\left(\frac{a_2+a_3-6a_4}{24}\right)^{5/2}+\frac{\alpha}{5184}(a_2+a_3-6a_4)\\(b_2+b_3-2b_1-2b_4-18b_{10})\end{array}\right]^{-1/5}, \tag{3.8e}$$

$$\sigma_{90}^C=\tau_Y\left[\left(\frac{a_1+a_2}{6}\right)^{5/2}+\alpha\left(\frac{a_1+a_2}{6}\right)\left(\frac{b_3+b_4}{27}\right)\right]^{-1/5}. \tag{3.8f}$$

In condition of equibiaxial tension, yielding occurs when $\sigma_{11}=\sigma_{22}=\sigma_b^T$, thus

$$\sigma_b^T=\tau_Y\left[\left(\frac{a_2+a_3}{6}\right)^{5/2}-\alpha\left(\frac{a_2+a_3}{6}\right)\left(\frac{b_2+b_3-2b_1-2b_4}{27}\right)\right]^{-1/5}. \tag{3.9}$$

While in condition of equibiaxial compression, yielding occurs when $\sigma_{11}=\sigma_{22}=\sigma_b^C$,

$$\sigma_b^C=\tau_Y\left[\left(\frac{a_2+a_3}{6}\right)^{5/2}+\alpha\left(\frac{a_2+a_3}{6}\right)\left(\frac{b_2+b_3-2b_1-2b_4}{27}\right)\right]^{-1/5}. \tag{3.10}$$

Furthermore, let r_θ be the ratio of transverse to through thickness increment of the logarithmic strain in condition of uniaxial loading directed at angle θ with x axis, then

$$r_\theta = -\frac{\sin^2\theta \frac{\partial\Phi}{\partial\sigma_{xx}} - \sin 2\theta \frac{\partial\Phi}{\partial\sigma_{xy}} + \cos^2\theta \frac{\partial\Phi}{\partial\sigma_{yy}}}{\frac{\partial\Phi}{\partial\sigma_{xx}} + \frac{\partial\Phi}{\partial\sigma_{yy}}}. \tag{3.11}$$

In particular,

$$\begin{aligned} r_0^T = & \left[a_1 \left(\frac{a_1+a_3}{6} \right)^{3/2} - \frac{2\alpha a_1(b_1+b_2)}{135} - \frac{\alpha b_1(a_1+a_3)}{45} \right] \\ & \times \left[a_3 \left(\frac{a_1+a_3}{6} \right)^{3/2} - \frac{2\alpha a_3(b_1+b_2)}{135} - \frac{\alpha b_2(a_1+a_3)}{45} \right]^{-1}, \end{aligned} \tag{3.12a}$$

$$\begin{aligned} r_{90}^T = & \left[a_1 \left(\frac{a_1+a_2}{6} \right)^{3/2} - \frac{2\alpha a_1(b_3+b_4)}{135} - \frac{\alpha b_4(a_1+a_2)}{45} \right] \\ & \times \left[a_1 \left(\frac{a_1+a_2}{6} \right)^{3/2} - \frac{2\alpha a_2(b_3+b_4)}{135} - \frac{\alpha b_3(a_1+a_2)}{45} \right]^{-1}, \end{aligned} \tag{3.12b}$$

$$\begin{aligned} r_0^C = & \left[a_1 \left(\frac{a_1+a_3}{6} \right)^{3/2} + \frac{2\alpha a_1(b_1+b_2)}{135} + \frac{\alpha b_1(a_1+a_3)}{45} \right] \\ & \times \left[a_3 \left(\frac{a_1+a_3}{6} \right)^{3/2} + \frac{2\alpha a_3(b_1+b_2)}{135} + \frac{\alpha b_2(a_1+a_3)}{45} \right]^{-1}, \end{aligned} \tag{3.12c}$$

$$\begin{aligned} r_{90}^C = & \left[a_1 \left(\frac{a_1+a_2}{6} \right)^{3/2} + \frac{2\alpha a_1(b_3+b_4)}{135} + \frac{\alpha b_4(a_1+a_2)}{45} \right] \\ & \times \left[a_1 \left(\frac{a_1+a_2}{6} \right)^{3/2} + \frac{2\alpha a_2(b_3+b_4)}{135} + \frac{\alpha b_3(a_1+a_2)}{45} \right]^{-1}. \end{aligned} \tag{3.12d}$$

In the above expressions, the superscripts "T" and "C" represent tension and compression conditions, respectively.

3.2 Numerical calculation of the anisotropy parameters

For a state of plane stress, the proposed yield function (Eq. (3.4)) contains 11 adjustable parameters $(a_1,\cdots,a_4)$, $(b_1,\cdots,b_5,b_{10})$ and α. Particularly, when $\sigma_{xy}=0$, the proposed criterion (Eq. (3.5)) has 8 adjustable parameters. In order to calibrate the anisotropy parameters in condition of plane stress, the following experimental data could be adopted: σ_0^T, σ_0^C, σ_{45}^T, σ_{45}^C, σ_{90}^T, σ_{90}^C, σ_b^T, σ_b^C, r_0^T, r_0^C, r_{45}^T, r_{45}^C, r_{90}^T, r_{90}^C. The choice of the reference yield stress is arbitrary. As a result, we may get the following set of 14 equations:

$$\left.\begin{array}{l}
\sigma_0^T(a_1,\cdots,a_4,b_1,\cdots,b_5,b_{10},\alpha)-\sigma_{ref}=0\\
\sigma_0^C(a_1,\cdots,a_4,b_1,\cdots,b_5,b_{10},\alpha)-\sigma_{ref}=0\\
\sigma_{45}^T(a_1,\cdots,a_4,b_1,\cdots,b_5,b_{10},\alpha)-\sigma_{ref}=0\\
\sigma_{45}^C(\sigma_{45}^C,a_1,\cdots,a_4,b_1,\cdots,b_5,b_{10},\alpha)-\sigma_{ref}=0\\
\sigma_{90}^T(\sigma_{90}^T,a_1,\cdots,a_4,b_1,\cdots,b_5,b_{10},\alpha)-\sigma_{ref}=0\\
\sigma_{90}^C(\sigma_{90}^C,a_1,\cdots,a_4,b_1,\cdots,b_5,b_{10},\alpha)-\sigma_{ref}=0\\
\sigma_b^T(\sigma_b^T,a_1,\cdots,a_4,b_1,\cdots,b_5,b_{10},\alpha)-\sigma_{ref}=0\\
\sigma_b^C(\sigma_b^C,a_1,\cdots,a_4,b_1,\cdots,b_5,b_{10},\alpha)-\sigma_{ref}=0\\
r_0^T(a_1,\cdots,a_4,b_1,\cdots,b_5,b_{10},\alpha)-r_{ref}=0\\
r_0^C(a_1,\cdots,a_4,b_1,\cdots,b_5,b_{10},\alpha)-r_{ref}=0\\
r_{45}^T(\sigma_0^T,a_1,\cdots,a_4,b_1,\cdots,b_5,b_{10},\alpha)-r_{ref}=0\\
r_{45}^C(\sigma_0^T,a_1,\cdots,a_4,b_1,\cdots,b_5,b_{10},\alpha)-r_{ref}=0\\
r_{90}^T(\sigma_0^T,a_1,\cdots,a_4,b_1,\cdots,b_5,b_{10},\alpha)-r_{ref}=0\\
r_{90}^C(\sigma_0^T,a_1,\cdots,a_4,b_1,\cdots,b_5,b_{10},\alpha)-r_{ref}=0
\end{array}\right\}. \tag{3.13}$$

$\sigma_0^T(\cdot)$, $r_0^T(\cdot)$, etc. are theoretical values calculated according to the formulae given in Section 3.1, while σ_{ref} and r_{ref} denote the corresponding experimentally determined yield stresses and r-values. The nonlinear equation system has 11 unknown anisotropy parameters $a_1,\cdots,a_4,b_1,\cdots,b_5,b_{10}$ and α. For the eight parameters version, less experiment data is necessary. In fact, greater or equal to eight equations are necessary to determine the adjustable parameters.

A traditional and convenient method to calculate the anisotropy parameters is to minimize the following error function by the least square method

$$\begin{aligned}
&\varepsilon(a_1,\cdots,a_4,b_1,\cdots,b_5,b_{10},\alpha)\\
=&\sum_i^n\lambda_i\left(1-\frac{(\sigma_\theta)_i^{th}}{(\sigma_\theta)_i^{\exp}}\right)^2+\sum_i^m\eta_i\left(1-\frac{(r_\theta)_i^{th}}{(r_\theta)_i^{\exp}}\right)^2\\
&+\mu\left(1-\frac{\left(\sigma_b^T\right)^{th}}{\left(\sigma_b^T\right)^{\exp}}\right)^2+\gamma\left(1-\frac{\left(\sigma_b^C\right)^{th}}{\left(\sigma_b^C\right)^{\exp}}\right)^2.
\end{aligned} \tag{3.14}$$

Here, "n" and "m" represent the number of experimental yield stresses and r-values, respectively for different orientations θ. The superscript indicates whether the respective value is experimental data or calculated results using the expressions as in Section 3.1 while λ_i, η_i, μ and γ are weight factors.

The next work is to optimize the anisotropy parameters $a_1,\cdots,a_4,b_1,\cdots,b_5,b_{10}$ and α, respectively, so as to get a minimum of the error function. There are different mathematical methods to solve such a problem. One can find a survey of such methods in [47].

The method of steepest descent is one of the most convenient methods, which will be adopted in this paper.

It is believed that the error minimization procedure discussed above is a great engineering method to examine a yield criterion's fexibility: a yield function is flexible enough for general purpose only if it can "pass" the error minimization procedure test [48]. In the following the new yield function will be applied to different materials to illustrate its predictive capability.

4 Applications

In order to check the proposed yield criterion's predictive ability and flexibility, in the following we will apply it to three different metallic materials: an HCP crystal structure magnesium, a shape memory alloy Cu-Al-Be and a Ni_3Al based intermetallic alloy. An important reason for choosing those materials is that their yield loci exhibit widely different shapes, which is preferred to check a yield function's flexibility.

4.1 Testing material AZ31 magnesium alloy

Andar et al. [49, 50] tested a commercial AZ31 magnesium alloy sheet under uniaxial tension-compression loading and proportional biaxial tensile loading using cruciform specimens. Bulge tests were also carried out to obtain a larger plastic strain than biaxial tension. Plastic work contours were determined over a range of equivalent plastic strain levels (0.4% $\sim$ 4%), to quantitatively determine the elastic-plastic deformation behavior. For details of experimental data, see Andar et al. [49]. The material data for the AZ31 Mg sheet material is given in Table 1. In order to calibrate the proposed yield function Eq. (3.5), the following data has been selected as input data: σ_0^T, σ_0^C, σ_{90}^T, σ_{90}^C, σ_b^T, r_0^T, r_0^C, r_{90}^T, r_{90}^C. Fig. 5 shows the yield loci of experiments of AZ31 Mg for different plastic strains, namely 0.4%, 0.8%, 2%, 4%, of the largest principal strain (experimental points are represented by symbols). The yield locus of the AZ31 Mg has a significant asymmetrical shape. Note that the yield stress in tension is much larger than that in compression ($\sigma_T/\sigma_C > 1.45$ for all cases). The asymmetry of yielding of magnesium is thought to be caused by the directionality of twinning [17]. AZ31 Mg also shows strong differential work hardening when subject to proportional biaxial stresses. This indicates that the measured work contours are different in both shape and scale. Fig. 5 also shows the theoretical yield loci of the proposed criterion given by Eq. (3.5). The parameters of the criterion were obtained by minimizing the error function (3.14) using the method of steepest descent. The calculated values of the parameters are given in Table 2. For the sake of comparison, yield loci predicted by Cazacu-Barlat (2004) [29] are also presented in Fig. 5. The coefficients for Cazacu-Barlat (2004), also calculated by the error minimization procedure, are given in Table 3.

It is observed that the predicted yield loci of the present theory and Cazacu-Barlat (2004) criterion are very close, and the main difference appears generally near equi-

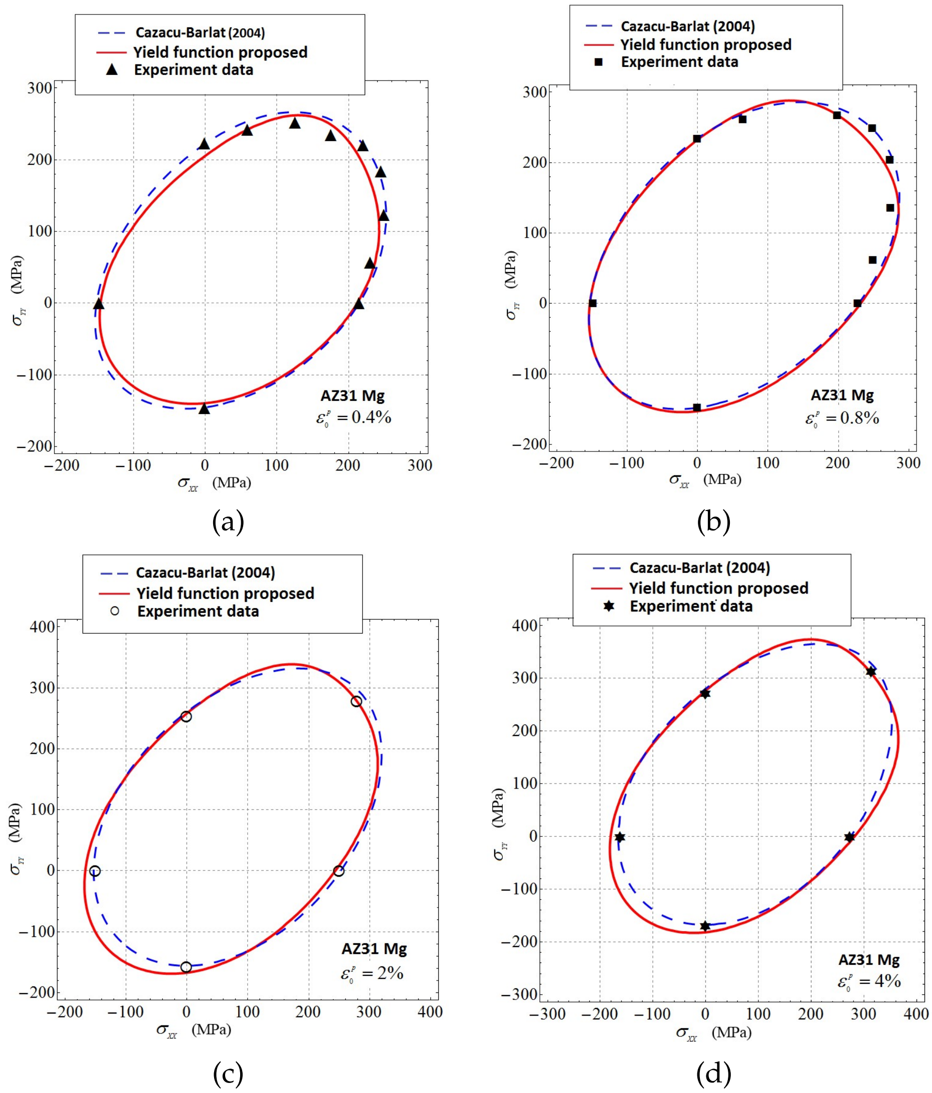

Figure 5: Experimentally determined yield loci of AZ31 Mg and yield loci predicted by the models of Cazacu-Barlat (2004) and the proposed criterion (data after Andar [49]).

biaxial tension or equi-biaxial compression area. Experimental results show that both theories can describe the asym-metric yield behavior of AZ31 Mg well at small plastic strain levels, although deviation between theory and experiment data exists for some points (see Figs. 5(a) and (b)). For larger strain levels, the biggest difference between Cazacu-Barlat (2004) criterion and the present theory appears near the equi-biaxial compression point (see Figs. 5(c) and (d)). For plastic strain of 2% and 4%, all five experiment points are used as input data to calibrate the yield functions, thus it's impossible to com-

Table 1: Experimental material data of AZ31 Mg.

ε_0^p	σ_0^T(MPa)	σ_0^C(MPa)	σ_{90}^T(MPa)	σ_{90}^C(MPa)	σ_b^T(MPa)	r_0^T(MPa)	r_0^C(MPa)	r_{90}^T(MPa)	r_{90}^C(MPa)	τ_Y*
0.004	215	-147	223	-146	221	0.382	0.141	0.715	0.158	124
0.008	228	-148	234	-148	245	0.59	0.141	0.951	0.158	132
0.02	250	-158	254	-162	279	2.56	0.141	3.35	0.158	144
0.04	274	-170	273	-173	315	2.56	0.141	3.35	0.158	158

* Approximated using $\tau_Y = \sigma_0^T/\sqrt{3}$.

Table 2: Anisotropic and tension-compression asymmetry coefficients of the proposed criterion for alloy AZ31 Mg.

ε_0^p	a_1	a_2	a_3	b_1	b_2	b_3	b_4	α
0.004	0.6559	3.131	2.8133	-0.1617	2.501	3.1041	-0.363	3.7115
0.008	0.6558	2.8938	2.8933	-0.2303	2.8637	2.8765	-0.2219	3.6205
0.02	0.6975	2.8239	2.8898	-0.2916	2.8255	2.8167	-0.1738	3.6585
0.04	0.6523	2.9515	2.9758	-0.1987	2.9751	2.9791	-0.2972	3.6858

Table 3: Anisotropic and tension-compression asymmetry coefficients of Cazacu-Barlat (2004) criterion for alloy AZ31 Mg.

ε_0^p	a_1	a_2	a_3	b_1	b_2	b_3	b_4	α
0.004	0.8231	2.4163	2.2614	-0.2443	2.3115	2.8206	-0.1892	2.3012
0.008	0.8659	2.6281	2.4868	-0.3412	2.5352	2.722	-0.1289	3.7736
0.02	0.5091	3.1601	3.3246	-0.4373	2.761	2.6397	-0.4261	3.7847
0.04	0.5328	3.2806	3.3675	-0.4451	2.7727	2.7445	-0.4471	3.8699

pare the prediction accuracy of the two models. One may also find that the theoretical yield loci do not match the experimental input data perfectly. If we use a Newton solver for calibration, the yield function will match the experimental input data perfectly. However, such an investigation is out of the scope of this paper since we are focusing on the flexibility aspects here.

4.2 Testing material Cu-Al-Be shape memory alloy

Shape memory alloy (SMA) often exhibits an asymmetric behavior between tension and compression. Bouvet et al. [51] conducted extensive experimental studies on the behavior of the Cu-Al-Be SMA under multiaxial proportional and nonproportional loadings. The initial yield surface of phase transformation initiation (austenite to martensite) was obtained. Fig. 6 shows the experimental initial transformation onset surface of Cu-Al-Be SMA (experiment data is plotted by symbols). Note that the transformation onset surface of Cu-Al-Be SMA has a significant asymmetrical shape, the compressive "yield" stress is 20% larger than tensile "yield" stress. Strictly speaking, the transformation onset surface of SMAs is different from the yield surface of metals. However, as both are boundaries of domain in stress space, it's reasonable to describe them with similar models. Herein we

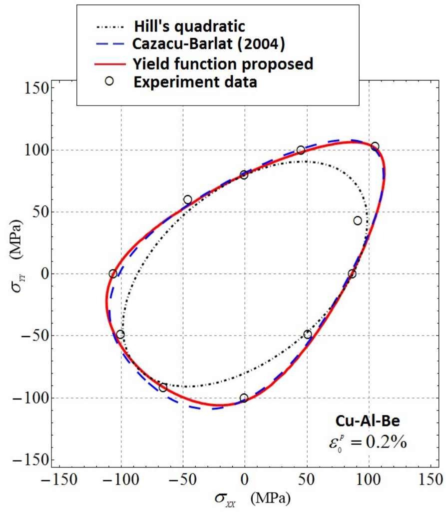

Figure 6: Experimentally determined yield loci of Cu-Al-Be SMA and yield loci predicted by the models of Hill's quadratic criterion, Cazacu-Barlat (2004) and the proposed criterion (data after Bouvet [50]).

will apply the proposed criterion to model the initial onset of transformation of Cu-Al-Be SMA.

Fig. 6 also shows the theoretical yield locus of the proposed criterion given by Eq. (3.5). The parameters for the proposed criterion, calculated using error minimization procedure, are listed in Table 4. For the sake of comparison, the yield loci of Hill's quadratic criterion [7] and Cazacu-Barlat (2004) criterion [29] are also potted in Fig. 6. The calculated coefficients of Cazacu-Barlat (2004) are given in Table 4, and the calculated anisotropic constants of Hill's quadratic criterion, denoted as F, G, H, are given in Table 5.

The predicted yield loci of Cazacu-Barlat (2004) and the proposed yield criterion for Cu-Al-Be are very close, and the main difference appears in biaxial compression area. Experiment results illustrate that the proposed yield function fits the experiment data

Table 4: Anisotropic and tension-compression asymmetry coefficients of yield criteria for Cu-Al-Be SMA.

Yield criterion	a_1	a_2	a_3	b_1	b_2	b_3	b_4	α
Proposed criterion	1.0497	1.307	1.0379	0.9256	0.8932	1.1147	1.299	-1.4713
Cazacu- Barlat (2004)	1.1047	1.1529	1.0471	0.6814	0.6028	0.8221	0.7803	-1.2109

Table 5: Calculated parameters of Hill's quadratic yield function for Cu-Al-Be SMA.

F	G	H
0.8827×10^{-4}	0.6414×10^{-4}	0.6798×10^{-4}

better than Cazacu-Barlat (2004). The proposed criterion can model the asymmetric transformation onset surface of Cu-Al-Be SMA very well except for the experiment point (91.43MPa, 42.86MPa), which seems like an experimental mistake. Cazacu-Barlat (2004) criterion over-values the yield stresses near equi-biaxial compression region a little bit. As Hill's quadratic criterion is based on the hypothesis of tension-compression symmetry, therefore it failed to reproduce the asymmetry shape of the transformation onset surface for Cu-Al-Be. Undoubtedly, modeling the plastic behavior of metals with remarkable tension-compression asymmetry by symmetric yield functions will cause significant errors.

4.3 Testing material Ni3Al based intermetallic alloy IC10

Next, we consider the experimental series of a Ni_3Al based super-alloy IC10, which was developed as blade materials in advanced aero-engine [52]. Due to the preferred $\langle 001 \rangle$ crystallographic orientation and tension-compression asymmetry of the Ll_2-long-range ordered Ni_3Al [28], the directionally solidified alloy exhibits both plastic anisotropy and yielding asymmetry between tension and compression. The author of the present paper [53] had studied the plastic behavior of IC10, and the yield locus according to 0.2% plastic strain of the largest principal strain was obtained by biaxial tensile tests on cruciform specimens and bi-compression tests on cubes. In Fig. 7 are presented the theoretical yield locus given by the proposed theory (Eq. (3.5)) together with the experimental data. The parameters involve in the 2D yield locus are given in Table 6. For the sake of comparison, yield loci predicted by Hill's quadratic criterion and Cazacu-Barlat (2004) are also presented in Fig. 7. The calculated coefficients for Cazacu-Barlat (2004) are given in Table 6, and the calculated anisotropic constants of Hill's quadratic criterion, denoted as F, G, H, are given in Table 7.

The yield loci of Cazacu-Barlat (2004) and the proposed yield criterion are very close and both can describe the asymmetric yield behavior of alloy IC10 well, except for few experiment points, which are overestimated by both theories. For Hill's quadratic criterion, signficant discrepancies are found in some stress states under biaxial compression. As discussed above, modeling the plastic behavior of metals with tension-compression asymmetry by symmetric yield functions will cause significant errors.

Table 6: Anisotropic and tension-compression asymmetry coefficients of yield criteria for alloy IC10.

Yield criterion	a_1	a_2	a_3	b_1	b_2	b_3	b_4	α
Proposed criterion	1.1392	1.2297	1.0684	0.939	0.6540	0.1318	-0.5981	0.9510
Cazacu-Barlat (2004)	1.1594	1.1673	1.1494	0.5941	0.5914	-0.4895	-0.4908	0.6727

Table 7: Calculated parameters of Hill's quadratic yield function for alloy IC10.

F	G	H
1.087×10^{-6}	0.5999×10^{-6}	0.869×10^{-6}

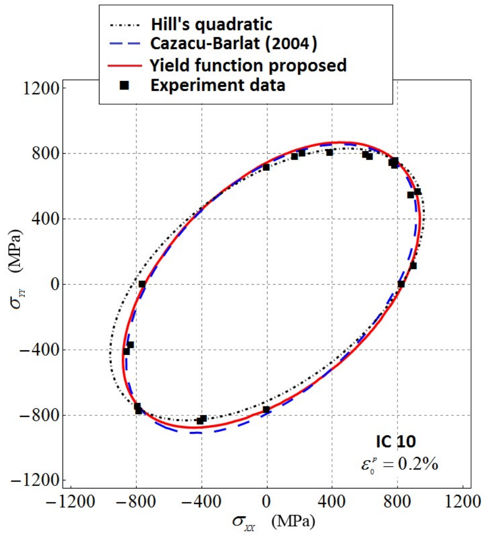

Figure 7: Experimental yield loci of alloy IC10 and yield loci predicted by the models of Hill's quadratic criterion, Cazacu-Barlat (2004) and the proposed criterion.

5 Conclusions

A new isotropic yield criterion which contains a product term of J_2 and J_3 is proposed. The isotropic criterion can model the yielding asymmetry of pressure insensitive metals. The main advantage of the proposed theory is that it leads to a good approximation of yield loci calculated by the Taylor-Bishop-Hill crystal plasticity model. Moreover, the proposed isotropic criterion is extended to orthotropy using the generalized invariants of the stress deviator. The parameters involve in the criterion are identified based on the error minimization method. In order to demonstrate the wide application of the proposed criterion, it is applied to different materials and compared with existing theories. Results show that the proposed theory can describe well the yielding behavior of AZ31 magnesium alloy and Ni3Al based super-alloy IC10. Furthermore, application to Cu-Al-Be SMA shows that the proposed theory can model the transformation onset of the shape memory alloy better than Cazacu-Barlat (2004) criterion, showing excellent predictive ability and flexibility.

Appendix: Discussion on the convexity of the proposed yield function

Convexity of yield surface should be satisfied in modeling the plastic behavior of metals. For yield function with simple expression, convexity of yield surface can be easily checked by assuming that its Hessian matrix is positive semi-definite. However, for

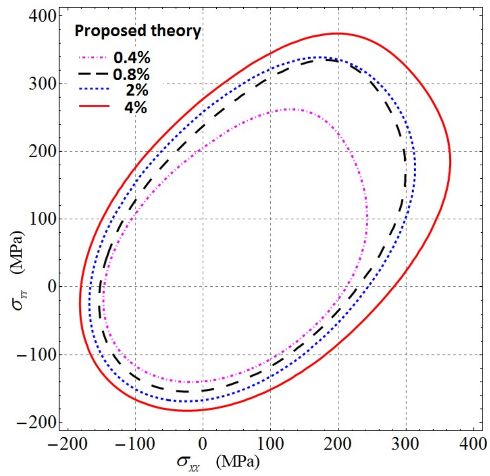

Figure 8: The calculated yield loci of AZ31 Mg by the proposed yield function at different plastic strains.

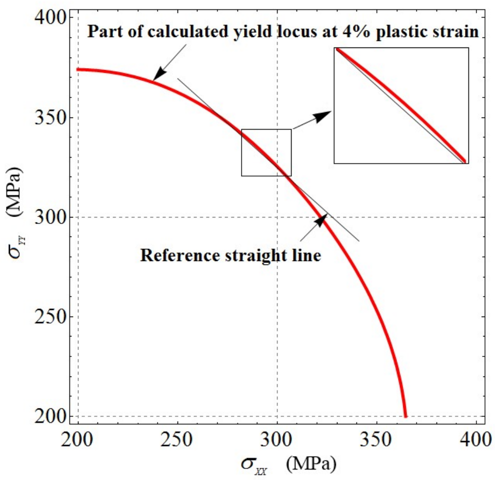

Figure 9: The zoomed segment of the yield locus of the proposed yield function for AZ31 Mg at 4% plastic strain.

anisotropic yield function containing more parameters with complex mathematical expression, the convexity requirement would not be easy to check. In this case, the convexity of yield criterion for a specific material can be investigated by graphical method. Khan et al. [54] have adopted this method to check the convexity of the extended Hill's quadratic yield criterion.

The convexity of the proposed yield function for the three different metallic materials applied in this study will be checked by graphical method. Let's start with alloy AZ31 Mg. From Fig. 8, it is observed that the curvature of the yield loci for AZ31 Mg reaches the smallest value near equibiaxial tension point for all strain levels. Fig. 9 shows the zoomed segment on the yield locus at 4% plastic strain near the equibiaxial tension point. In order to check the convexity of yield locus near this area, a reference straight line has been plotted. It can be observed that segments of the yield locus with the smallest curvature is convex. This indicates that the whole yield locus of AZ31 Mg at 4% plastic strain is convex. By applying the same method to other strain levels, the yield loci obtained with plastic strain lower than 4% can also satisfy the condition of convexity. Therefore, the convexity of the proposed yield function for AZ31 Mg can be satisfied in engineering applications.

By applying the same method to other materials, it shows that the convexity of the proposed yield function for Cu-Al-Be SMA and Ni3Al based alloy IC10 can be satisfied in engineering applications too.

Acknowledgements

Lei Chen is grateful for the financial support for this work by the Natural Science Foundation of Jiangsu Province, China (Grant No. BK20160486). Jian Zhang is grateful for the financial support from the National Natural Science Foundation of China (Grant No. 11872190). Six Talent Peaks Project in Jiangsu Province (Grant No. 2017-KTHY-010) and Research Start-Up Foundation for Jinshan Distinguished Professorship at Jiangsu University (Grant No. 4111480003).

References

[1] D. Banabic, Sheet Metal Forming Processes: Constitutive Modelling and Numerical Simulation, Springer Heidelberg, Dordrecht, London New York, (2010).
[2] H. Yang, X. G. Fan, and Z. C. Sun et al., *Recent developments in plastic forming technology of titanium alloys,* Sci. China. Tech. Sci., 54 (2011), pp. 490–501.
[3] F. F. Zhang, J. S. Chen, and J. Chen et al., *Review on development and experimental validation for anisotropic yield criterions (in Chinese),* Adv. Mech., 42 (2012), pp. 68–80.
[4] D. C. Drucker, *Relation of experiments to mathematical theories of plasticity,* J. Appl. Mech., 16 (1949), pp. 349–357.
[5] A. V. Hershey, *The plasticity of an isotropic aggregate of anisotropic face centered cubic crystals,* J. Appl. Mech. Trans. ASME, 21 (1954), pp. 241–249.
[6] M. H. Yu, L. N. He, and L. Y. Song, *Twin shear stress strength theory and its generalization (in Chinese),* Sci. China. Ser A, 12 (1985), pp. 1113–1120.
[7] R. Hill, *A theory of the yielding and plastic flow of anisotropic metals,* Proc. Soc. London. A, 193 (1948), pp. 281–297.
[8] D. Banabic, Anisotropy of Sheet Metals, Springer-Verlag, Berlin Heidelberg, New York, (2000).
[9] M. H. Yu, *Advances in strength theories for materials under complex stress state in the 20th Century,* Appl. Mech. Rev., 55 (2002), pp. 198–218.

[10] R. HILL, *Theoretical plasticity of textured aggregates,* Math. Proc. Camb. Phil. Soc., 85 (1979), pp. 179–191.

[11] R. HILL, *Constitutive modelling of orthotropic plasticity in sheet metals,* J. Mech. Phys. Solids, 38 (1990), pp. 405–417.

[12] R. HILL, *A user-friendly theory of orthotropic plasticity in sheet metals,* Int. J. Mech. Sci., 35 (1993), pp. 19–25.

[13] R. HILL, S. S. HECKER, AND M. S. STOUT, *An investigation of plastic flow and differential work hardening in orthotropic brass tubes under fluid pressure and axial load,* Int. J. Solids. Struct., 31 (1994), pp. 2999–3021.

[14] W. F. HOSFORD, *Texture strengthening,* Metals. Eng. Quart., 6 (1966), pp. 13–19.

[15] W. F. HOSFORD, *A generalized isotropic yield criterion,* J. Appl. Mech., 39 (1972), pp. 607–609.

[16] W. F. HOSFORD, AND T. J. ALLEN, *Twining and directional slip as a cause for strength differential effect,* Met. Trans., 4 (1973), pp. 1424–1425.

[17] W. F. HOSFORD, The Mechanics of Crystals and Textured Polycrystals, Oxford University Press, New York, (1993).

[18] F. BARLAT, AND J. LIAN, *Plastic behavior and stretchability of sheet metals. Part I: Yield function for orthotropic sheets under plane stress conditions,* Int. J. Plast., 5 (1989), pp. 51–66.

[19] F. BARLAT, D. J. LEGE, AND J. C. BREM, *A six-component yield function for anisotropic materials,* Int. J. Plast., 7 (1991), pp. 693–712.

[20] F. BARLAT, J. C. BREMA, AND J. W. YOON ET AL., *Plane stress yield function for aluminum alloy sheets—part 1: theory,* Int. J. Plast., 19 (2003), pp. 1297–1319.

[21] F. BARLAT, J. N. YOON, AND O. CAZACU, *On linear transformations of stress tensors for the description of plastic anisotropy,* Int. J. Plast., 23 (2007), pp. 876–896.

[22] L. B. XIN, G. S. DUI, AND S. Y. YANG ET AL., *Elastic-plastic analysis for functionally graded thick-walled tube subjected to internal pressure,* Adv. Appl. Math. Mech., 8 (2016), pp. 331–352.

[23] Z. Y. CAI, M. WAN AND Z. G. LIU ET AL., *Approximate method formulating plastic potentials of porous sheet metals with non-quadratic anisotropy,* Int. J. Mech. Sci., 123 (2017), pp. 198–213.

[24] H. B. WANG, W. ZHOU AND Y. YAN ET AL., *Parameter determination method of Gotoh yield criterion based on non-associated flow rule,* China J. Theor. Appl. Mech., 50 (2018), pp. 1051–1062.

[25] W. C. LIU. B. K. CHEN, AND Y. PANG, *Numerical investigation of evolution of earing, anisotropic yield and plastic potentials in cold rolled FCC aluminum alloy based on the crystallographic texture measurements,* Euro. J. Mech. A/Solids, 75 (2019), pp. 41–55.

[26] Y. S. LOU, AND J. W. YOON, *Alternative approach to model ductile fracture by incorporating anisotropic yield function,* Int. J. Solids. Struct., 164 (2019), pp. 12–24.

[27] X. S. WANG, W. L. HU, AND S. J. HUANG, ET AL., *Experimental investigations on extruded 6063 aluminum alloy tubes under complex tension-compression stress states,* Int. J. Solids. Struct., 168 (2019), pp. 123–137.

[28] S. S. EZZ, D. P. POPE, AND V. PAIDAR, *The tension/compression flow stress asymmetry in* Ni_3*(Al, Nb) single crystals,* Acta. Metall., 30 (1982), pp. 921–926.

[29] O. CAZACU, AND F. BARLAT, *A criterion for description of anisotropy and yield differential effects in pressure-insensitive metals,* Int. J. Plast., 20 (2004), pp. 2027–2045.

[30] O. CAZACU, B. PLUNKETT, AND F. BARLAT, *Orthotropic yield criterion for hexagonal close packed metals,* Int. J. Plasticity, 22 (2006), pp. 1171–1194.

[31] O. CAZACU, R. I. IOAN, AND W. Y. JEONG, *Orthotropic strain rate potential for the description of anisotropy in tension and compression of metals,* Int. J. Plasticity, 26 (2010), pp. 887–904.

[32] Y. S LOU, H. HUH, J. W. YOON, *Consideration of strength differential effect in sheet metals with*

symmetric yield functions, Int. J. Mech. Sci., 66 (2013), pp. 214–223.

[33] O. CAZACU, AND J. B. STEWART, *Analytical criterion for porous solids containing cylindrical voids in an incompressible matrix exhibiting tension-compression asymmetry,* Philos. Mag., 93 (2013), pp. 1520–1548.

[34] R. K. VERMA, T. KUWABARA, AND K. CHUNG ET AL., *Experimental evaluation and constitutive modeling of non-proportional deformation for asymmetric steels,* Int. J. Plast., 27 (2011), pp. 82–101.

[35] D. STEGLICH, W. BROCKS, AND J. BOHLEN ET AL., *Modeling direction-dependent hardening in magnesium sheet forming simulations,* Int. J. Mater Form., 4 (2011), pp. 243–253.

[36] M. N. MEKONEN, D. STEGLICH, AND J. BOHLEN ET AL., *Mechanical characterization and constitutive modeling of Mg alloy sheets,* Mater. Sci. Eng. A, 540 (2012), pp. 174–186.

[37] M. O. ANDAR, T. KUWABARA, AND D. STEGLICH, *Material modeling of AZ31 Mg sheet considering variation of r-values and asymmetry of the yield locus,* Mater. Sci. Eng. A, 549 (2012), pp. 82–92.

[38] O. CAZACU, *New yield criteria for isotropic and textured metallic materials,* Int. J. Solids. Struct., 139-140 (2018), pp. 200–210.

[39] A. R. RAJAB, AND S. E. BAYAOUMI, Fundamentals and Applications, CRC Press LLC, (1999).

[40] G. I. TAYLOR, AND H. QUINNEY, *The plastic distortion of metals,* Philos. Trans. R. Soc. A, 230 (1931), pp. 323–362.

[41] J. W. F. BISHOP, AND R. HILL, *A theoretical deviation of the plastic properties of a polycrystalline face-centered metal,* Philos. Mag. Ser., 42 (1951), pp. 1298–1307.

[42] Z. SOBOTKA, *The fundamental relations of theory of plasticity and a new concept of the plastic potential for the anisotropic materials,* Stavebnicky, Casopsis XIV, pp. 373–380.

[43] J. P. BOEHLER, AND A. SAWCZUK, *Equilibre limite des sols anisotropes,* J. Mecanique., 9 (1970), pp. 5–33.

[44] A. P. KARAFILLIS, AND M. C. BOYCE, *A general anisotropic yield criterion using bounds and a transformation weighting tensor,* J. Mech. Phys. Solids, 41 (1993), pp. 1859–1886.

[45] O. CAZACU, AND F. BARLAT, *Generalization of Drucker's yield criterion to orthotropy,* Math. Mech. Solids. 6 (2001), pp. 613–630.

[46] Q. HU, X. F. LI AND X. H. HAN ET AL., *A normalized stress invariant-based yield criterion: Modeling and validation,* Int. J. Plast., 99 (2017), pp. 248–273.

[47] W. ALT, Nichtlineare Optimierung, Vieweg Verlag, (2002).

[48] H. ARETZ, *A nonquadratic plane stress yield function for ortho-tropic sheet metals,* J. Mater. Proces. Tech., 168 (2005), pp. 1–9.

[49] M. O. ANDAR, T. KUWABARA, AND D. STEGLICHC, *Material modeling of AZ31 Mg sheet considering variation of r-values and asymmetry of the yield locus,* Mater. Sci. Eng. A, 549 (2012), pp. 82–92.

[50] M. O. ANDAR, T. KUWABARA, AND D. STEGLICHC, *Description of Anisotropy and yield differential effects for AZ31 Mg sheet using Cazacu 2004 yield criterion,* J. JSEM, Special Issue, 12 (2012), pp. 151–156.

[51] C. BOUVET, S. CALLOCH, AND C. LEXCELLENT, *Mechanical behavior of a Cu–Al–Be shape memory alloy under multiaxial proportional and non-proportional loadings,* J. Eng. Mater. Tech., 124 (2002), pp. 112–124.

[52] X. H. ZHAO, Z. H. HUANG, AND Y. N. TAN ET AL., *New Ni3Al-based direction-ally-solidified superalloy IC10,* J. Aeronaut. Mate., 26 (2006), pp. 20–24.

[53] L. CHEN, W. D. WEN, AND H. T. CUI, *Measurement and analysis of yield locus of superalloy*

IC10 under biaxial tension, Acta. Aeronaut. Astronaut. Sin., 33 (2012), pp. 77–84.

[54] A. S. KHAN, S. J. YU, AND H. W. LIU, *Deformation induced anisotropic responses of Ti–6Al–4V alloy Part II: A strain rate and temperature dependent anisotropic yield criterion,* Int. J. Plast., 7 (2012), pp. 14–26.